

COVID-19 Status Forecasting Using New Viral variants and Vaccination Effectiveness Models

Essam A. Rashed^{1,2}, PhD, Sachiko Kodera¹, PhD, Akimasa Hirata^{1,3}, PhD

¹ *Department of Electrical and Mechanical Engineering, Nagoya Institute of Technology, Nagoya 466-8555, Japan*

² *Department of Mathematics, Faculty of Science, Suez Canal University, Ismailia 41522, Egypt*

³ *Center of Biomedical Physics and Information Technology, Nagoya Institute of Technology, Nagoya 466-8555, Japan*

Corresponding Author: Essam A. Rashed
Gokiso-cho, Showa-ku, Nagoya 466-8555, Japan
Nagoya Institute of Technology, Japan
email: essam.rashed@nitech.ac.jp
Tel: +81-52-735-7916

Summary

Background: Recently, a high number of daily positive COVID-19 cases have been reported in regions with relatively high vaccination rates; hence, booster vaccination has become necessary. In addition, infections caused by the different variants and correlated factors have not been discussed in depth. With large variabilities and different co-factors, it is difficult to use conventional mathematical models to forecast the incidence of COVID-19.

Methods: Machine learning based on long short-term memory was applied to forecasting the time series of new daily positive cases (DPC), serious cases, hospitalized cases, and deaths. Data acquired from regions with high rates of vaccination, such as Israel, were blended with the current data of other regions in Japan to factor in the potential effects of vaccination. The protection provided by symptomatic infection was also considered in terms of the population effectiveness of vaccination as well as the waning protection and ratio and infectivity of viral variants. To represent changes in public behavior, public mobility and interactions through social media were also included in the analysis.

Findings: Comparing the observed and estimated new DPC in Tel Aviv, Israel, the parameters characterizing vaccination effectiveness and the waning protection from infection were well estimated; the vaccination effectiveness of the second dose after 5 months and the third dose

after two weeks from infection by the delta variant were 0.24 and 0.95, respectively. Using the extracted parameters regarding vaccination effectiveness, new cases in three prefectures of Japan were replicated.

Interpretations: The key factor influencing the prevention of COVID-19 transmission is the vaccination effectiveness at the population level, which considers the waning protection from vaccination rather than the percentage of fully vaccinated people. The threshold of the efficiency at the population level was estimated as 0.3 in Tel Aviv and 0.4 in Tokyo, Osaka, and Aichi. Moreover, a weighting scheme associated with infectivity results in more accurate forecasting by the infectivity model of viral variants.

Funding: This work was conducted as a part of Project COVI-19 AI and Simulation under the Cabinet Secretariat, Japan (data sharing without funding). The expenses were covered by general funding from the Ministry of Education, Culture, Sports, Science and Technology, Japan, for the center of Biomedical Physics and Information Technology, Nagoya Institute of Technology (director: AH).

Keywords: COVID-19; forecasting; deep learning; vaccination effectiveness

Research in context

Evidence before this study: Before the COVID-19 pandemic, mathematical models, such as the Susceptible, Exposed, Infectious, and Recovered model and its extensions, were used to estimate the rate of viral transmission. Due to the global transmission of this new virus, a more sophisticated forecasting model based on machine learning approaches is necessary. However, based on a review search using SCOPUS and Web of Science, long-term forecasting and projection models that consider vaccination effectiveness and different viral variants have not been developed. The search strategy we conducted is included in the Supplementary Materials.

Added value of this study: Previously, it was possible to estimate new positive cases using few factors in a mathematical manner. After large-scale vaccination campaigns and the emergence of different viral variants, the estimation has become complicated. There are two points where the prediction is not straightforward: the timing of the infection upsurge and the potential protection through vaccination. The infection upsurge can be determined by including parameters regarding the infectivity index. For protection conferred by vaccination, real world information is limited.

However, applying the epidemic tendencies of one country to others may not always be successful as epidemics have different patterns of spread in different regions. To overcome this complication, we developed a deep learning approach comprised of two networks; one that extracts the parameters associated with vaccination effectiveness and another that applies the effects of vaccination from regions with high vaccination rates. With this combination, we succeeded in demonstrating the COVID-19 status of different prefectures in Japan.

Implications of all the available evidence: The vaccination rate was not a sufficient representation of the vaccination effectiveness; thus, learning the vaccination effectiveness explicitly through deep learning models was informative. The two models work well during the early phases of vaccination. The proposed framework may also assist in learning about vaccination effectiveness and the waning protection of vaccination, which can be the basis of future vaccination strategies and policies during future pandemics.

Introduction

The emergence of Coronavirus Disease-2019 (COVID-19) in late 2019 resulted in several changes in the daily routine of people and has become a significant cause of mortality worldwide, causing more than 5.5 million deaths (<https://covid19.who.int>). Due to vaccination, the number of daily positive cases (DPC) has decreased in several countries. Although some countries have achieved high vaccination rates, other countries are far behind, with only a small proportion of their respective populations being vaccinated. This is mainly due to the lack of resources¹, vaccination hesitancy², or other related issues. While mass immunization has been reported in several countries³, vaccination rates are not high enough in others.

One of the first countries to vaccinate its population was Israel; however, relatively high DPCs were reported in August 2021 despite the country's vaccination rate being above 68%⁴. One reason for this upsurge was attributed to the high interactivity of the Delta variant⁵ and the waning protection from vaccination⁶, especially for those who have been vaccinated very early during the pandemic⁷. A similar trend was observed in the United Kingdom⁸ and the United States⁹. The data obtained from countries with high vaccination rates would be useful in predicting the future potential in follow-up regions. However, it is difficult to manipulate data acquired from other regions considering the variations of the different influencing factors.

Several national and regional projects are currently in progress to predict the status of the COVID-19 pandemic^{10,11}. The aim of such projects is to understand the pandemic data to improve medical resource allocation, intervention, and policy settings. Susceptible, Exposed, Infectious, and Recovered (SIR or SEIR) models have often been used to solve these problems^{12,13}, and several recent studies have demonstrated the robust abilities of machine learning approaches to

adjust for realistic scenarios without forming strict assumptions¹⁴. In contrast, earlier studies did not consider the public's mobility¹⁵, which has been clarified as a dominant factor characterizing new cases as a surrogate marker for social distancing^{16,17}. In addition, the forecasts were limited to only a few days¹⁸. Recently, several studies have considered the data pattern change due viral variants, and we have underlined the difficulty of predicting when new variants will appear¹⁹. It is critical for any successful model to be able to predict the beginning of a new wave of infections and its potential magnitude. The difficulty in modeling the upsurge of cases may also be attributed to behavioral changes when the DPC are low.

Although conventional projection strategies did not thoroughly consider the effects of vaccination, some studies did²⁰. With the emergence of messenger RNA vaccines, the efficiency of vaccination in protecting against infection will dramatically improve. The weekly incidence of COVID-19 since administering the first vaccine dose started to decrease after two weeks, which further decreased after four weeks²¹. After the second dose, vaccine effectiveness reached 75%–95% after a few weeks^{22,23}. However, vaccine efficiency may depend on the dominant viral variant²². For the Pfizer-BioNtech vaccine, its efficacy for health-care workers has been extensively examined²¹ and complete vaccination is defined as two doses given 21 days apart. Therefore, data from regions with high vaccination rates and new variants may serve as important guides for forecasting potential risks in other regions.

Here, we propose an efficient method to forecast the COVID-19 status of one area based on viral variant modeling and vaccination effectiveness using a framework for data projection obtained from other regions. The proposed approach, which was based on insights and data from regions that have achieved high vaccination rates, can help optimize vaccination requirements in regions with low vaccination rates. Considering that more than 65% of countries still have vaccination rates below 70% (10 Jan. 2022, WHO), these countries may apply protocols from other countries that have achieved high vaccination rates. Moreover, the developed model can provide a clearer understanding of potential booster shot requirements and when they should be administered.

Methods

Forecasting model

The forecasting model was designed using a multi-path long short-term memory (LSTM) neural network based on our earlier study detailed in (19). The main difference of LSTM from conventional methods such as SIR/SEIR is that in the deep learning model, the number of variables (network features) are extremely large and can handle data non-linearity in a more efficient manner. The network parameters are optimized based on an ablation study¹⁹. The main data stream of the forecasting model and fine details on the training and testing phases are shown

in Figure 1. Training is implemented through a set of networks, with each network trained to forecast a single COVID-19 status indicator (DPC, serious cases [SC], hospitalized cases [HC], daily death cases [DC], and daily hospital discharged cases [CC]). The testing phase is considered with the updated concurrent data for long term forecasting. In other words, the input network data are updated using the current estimate for future forecasting, as shown in Figure S1.

Adaptation model

The projection of the epidemic tendency in one country to other countries is not always successful as epidemic parameters and associated factors in different countries may not be consistent. The two neural networks work well especially during the early stages of vaccination when the effects of vaccination are still unclear. The adaptation model is trained using a simplified combination of data wherein the target must learn the effects of vaccination within different stages of the pandemic. With this design, we can think of the “forecasting model” as the local scope network and the “adaptation model” as the global scope network. This strategy can efficiently enable the use of data of countries with high vaccination rates without considering local features. The data flow between the forecasting and adaptation models is shown in Figure 1 (c).

Vaccination effectiveness at population level

As the vaccination rate may not reflect the actual efficiency due to the variations in vaccines and waning protection over time⁷, we proposed a representation of vaccination protection, which is defined as the vaccination effectiveness at the population level that considers the waning protection. The vaccination effectiveness at the population level in each city or prefecture was assumed to be as follows:

$$E(d) = \sum_{t=1}^T \sum_{i=0}^d (N_t(d-i) \cdot e_t(i))/P, \quad (1)$$

$$e_t(i) = \begin{cases} a_t \cdot i/K & (i \leq K), \\ a_t - s(i-K) & (i > K), \end{cases} \quad (2)$$

where d is the day index and n_t denotes the number of people newly administrated with the vaccine t . e_t is the individual vaccination effectiveness on i days after inoculation. Parameters a and s are adjusted to reach a vaccination effectiveness peak within K days after inoculation, which then decrease linearly. P is the deemed population expressed as the summation of the population of the entire prefecture and the cumulative number of the second and third doses. Here, we assumed $T = 3$ to demonstrate the number of vaccine doses (vaccines with a single dose, such as that of Johnson & Johnson, was not considered here) and $K = 14$ for the two-week latency period of the vaccination effect. The parameters of a_1 and a_2 for the Delta variant were chosen as 0.605 and 0.756, respectively, both of which are based on a meta-analysis of

systematic reviews (11 study groups)²². The parameters coincide with the reported real-world vaccination effectiveness²⁴. The parameters of s and a_3 are computed as explained below. The antibody levels of infected people are comparable to or somewhat lower than those of fully vaccinated persons²⁵; thus, the DPC is counted as additional value of fully vaccinated people.

Infectivity of viral variant

Different viral variants and mutations have been reported during the recent waves of infection of COVID-19. In addition, different variants have different rates of spread, infectivity, and resistance to the currently administered vaccines. This effect has become significant since the emergence of the Delta and Omicron variants. Therefore, developing an infectivity model based on the dominant (or partially spreading) variant is necessary. The normalized infectivity index (\tilde{f}_i) is computed using the following equation:

$$\tilde{f}(d) = (\alpha - \beta) \frac{f(d) - \min(f)}{\max(f) - \min(f)} + \alpha \quad (3)$$

$$f(d) = \sum_{j=1}^N \omega_j v_{d_j} \quad \forall d \quad (4)$$

where v_{d_j} is the percentage of variant j at day d , ω_j is a weighting parameter assigned to each variant that demonstrates its relative infectivity, and parameters α and β are scaling parameters. As variant data were reported weekly, daily values were computed using linear interpolation.

Validation measurements

For quantitative evaluation, the average relative error over a period of N days was computed as follows:

$$Error = \frac{1}{N} \sum_{d=1}^N \frac{|y_d - \hat{y}_d|}{y_d} \quad (5)$$

where y_d and \hat{y}_d are the real and estimated positive cases on day d , respectively.

Data

The data combination used in the forecasting model includes the (i) current COVID-19 parameters (DPC, SC, HC, DC and CC), (ii) mobility data (retail & recreation, grocery & pharmacy, parks, transit stations, workplaces, and residences), (iii) meteorological data (daily maximum and minimum temperatures and daily average humidity), (iv) day labels (working days or holidays [i.e., weekends or national holidays]), (v) viral variant infectivity, and (vi) vaccination effectiveness. The main difference of this model from that from our previous study is that serious cases, hospitalized

cases, and deaths were considered in item (i) in addition to items (v) and (vi). In addition, in the analysis of Tokyo, Osaka, and Aichi, the number of tweets and population at night were considered, which are potentially related to changes in public behavior. The effectiveness of the latter can be reported in (27). The breakdown and definition of each dataset are listed in Table S1. Vaccination data, along with current COVID-19 data, were collected from external regions (Tel Aviv, Israel).

Input Data for Japan

The COVID-19 data of Tokyo were obtained from online open sources maintained by the Japanese Ministry of Health, Labor, and Welfare (MHLW) (28). Mobility data were downloaded from the global Google mobility reports (<https://www.google.com/covid19/mobility/>). Meteorological data were obtained from the Japan Meteorological Agency (<https://www.jma.go.jp/jma/indexe.html>). Day labels were based on the Japanese calendar, which were assigned as 1/0 for working/vacation days, respectively. Official state-of-emergency declarations by the Japanese government were assigned as 1/0 for active/inactive status, respectively. Information about the dominant variant was obtained from official MHLW reports (https://www.mhlw.go.jp/stf/seisakunitsuite/newpage_00054.html). Vaccination rates were obtained from the Government CIO's Portal, Japan (https://cio.go.jp/c19vaccine_opendata).

Social networking data were obtained from Twitter, and mobility at downtown areas were computed as the nighttime population who stayed near restaurants and bars. Twitter data were used as it may indicate social activities where close contact occurs, and the downtown population was considered as several domestic reports have indicated that the main infection clusters may be due to close contacts in these areas. Tweets with keywords “BBQ,” “drinking party”, and “karaoke” (in Japanese) were chosen as risk-related terms. Data were obtained from NTT Data, INC. and processed by Toyoda Lab., University of Tokyo and shared through the Cabinet Secretariat COVID-19 AI Simulation Project¹⁰. When determining the number of tweeted keywords, those completed during the day or the previous day, or those planned until the next day, were extracted. For corresponding tweets, information on the prefecture was extracted from the user's address. Note that due to the limited number of tweets, we only focused on three prefectures (Tokyo, Osaka, and Aichi); the number of tweets in other prefectures was generally lower, and the required number of tweets from other prefectures was not obtained. This is one reason why the analysis focused on these prefectures only.

Three (Tokyo), two (Osaka), and one (Aichi) metropolitan areas were selected to represent the downtown districts with restaurants and bars (mesh size of 500 m × 500 m area) (see Supplemental Material for more detail).

Input Data for Tel Aviv

The COVID-19 data and vaccination rate in Tel Aviv were obtained from online open sources (<https://info.data.gov.il/datagov/home/>), and mobility data were obtained from Google mobility reports. The average interval between the administration of the first and second doses was assumed as three weeks.

Scenarios

Optimize vaccination effectiveness using Tel Aviv data

The vaccination effectiveness calculated from Eq. (1) represents the model of protection from infection resulting from vaccination. With a variety of vaccines and other policy variables, parameters a_t and s should be adjusted based on real local data. For this purpose, we replicated the DPC in Tel Aviv and adjusted the parameters. Tel Aviv was selected as it has a high vaccination rate and shared similarities with the vaccines used in Tokyo (BNT162b2). We then investigated three values for s (0.21, 0.24, and 0.27), which characterizes the waning protection from vaccines, and the efficiency of the third dose (booster) was represented by a_3 (0.75, 0.85, and 0.95). The duration of vaccine effectiveness is plotted in Figure 2. A verification study using training data from August 1, 2020 to July 30, 2021 and testing data from August 1 to September 23, 2021 was conducted to estimate s and a_3 . The optimum a_3 value was 0.95, which is consistent with that in the report of Pfizer and BioNTech²⁶. Also, the slope of the waning protection was 0.24, which agrees with large scale study⁹.

Exploring different input parameters for Tokyo, Osaka, and Aichi

We then explored parameters which will correlate well with the new DPC. The main factors that might potentially influence the DPC in the future are listed in Table S1. The viral variant is essential and can be extracted from the data in different countries, and the day label of "holiday" is potentially related to behavioral changes; both of which can be easily defined with any uncertainty, thus their use as the default parameters. There are different categories for mobility, including those in different urban regions. In our previous study, we have shown that in most prefectures, mobility at transit stations is an essential parameter, whereas remaining is also related to public activities in different urban regions. In addition, the nighttime population can identify social activities in regions where infection clusters were reported, which we compared using a new set of input parameters. Although weather was suggested to correlate with the number of DPC in some studies, others have denied this²⁷. In this study, temperature and humidity, which are also related to the absolute humidity, were considered simultaneously. The vaccination effect was considered in the adaption of the neural network. To demonstrate the effectiveness of our proposed

forecasting system, we applied the same scenarios for Tokyo to Osaka and Aichi. Input parameter optimization was then conducted to validate the accuracy of forecasts.

Results

Extraction of parameters characterizing the waning protection from vaccination and third dose

The parameters in Eq. (1) were revised to replicate new DPC in Tel Aviv. From Figure 2, the observed and replicated DPC were in agreement when s and a_3 were set to 0.27 and 0.95, respectively. The average residual error of DPC from August 27 to November 21, 2021 was 0.289. Considering the incubation period (7–10 days), the efficiency of vaccination at the population level ranged from 0.29 to 0.32. It is clear from the data presented in Figure 2 (c) that different vaccination models will lead to different estimations of the DPC.

Input parameters for DPC

After considering all input parameters, an extensive sensitivity study was conducted to minimize the input datasets. First, a single item was selected from each data set to minimize the total forecasting error. The seven selected inputs were then optimized to minimize possible number based on error. It was found that the optimized data inputs are those corresponded to the current DPC, mobility (transit station), model of the viral variant, twitter data (“nomikai”), and vaccination effectiveness. The variant infectivity computed for Tokyo is shown in Figure S2, with different weighting factors assigned to different viral variants. Figure 3 shows the estimated DPC for the given parameters in Tokyo. The first set was generated using all datasets whereas the second estimation was obtained using optimized data which matched with the most accurate observed values. As shown in Table 1, the estimated DPC in Tokyo had error values of 0.23, 0.09, 0.78, and 0.36 for the spread, peak, decay, and all phases, respectively. The corresponding values for Osaka and Aichi were 0.24, 0.09, 0.41, 0.24, and 0.13, 0.16, 0.21, 0.17, respectively, which are highly consistent with the data of Tokyo. These results demonstrate that the viral variants model plays an important role during the spread phase in terms of starting time and peak value. In addition, the vaccination effectiveness model clearly contributes to the decay phase and can correctly forecast the rapid decay presented in the fifth COVID-19 wave in Japan. Figure S3 demonstrates forecasting during a pandemic state wherein positives, serious cases, hospitalized cases, deaths, and hospital dispatch cases for Tokyo, Osaka, and Aichi are forecasted.

Adaptation of vaccination effectiveness modeling

The estimation of new DPC using the combination of forecasting and adaptation models is shown in Figure 4. With the forecasting model alone, the spreading phase was highly consistent

with real data; however, the decay phase was not. On the other hand, the combination of the two models resulted in more accurate results, especially in the decay phase, due to the application of the vaccination effectiveness acquired from the Tel Aviv data. The difference between the two models in the spread phase was marginal; however, it was significant in the decay phase. This tendency is similar to that of our previous study wherein the adaptation of new viral variants was discussed¹⁹. We found that different combinations of data as well as different time frames would lead to significant changes in the results, especially those for the long-term forecasting. For example, in the early stages of the pandemic and prior to the emergence of viral variants, the meteorological data was suggested to highly correlate with the incidence of infection²⁷. However, when new factors, such as vaccination effectiveness and viral variant infectivity, were considered, the importance of meteorological data was lessened. Table 1 demonstrates a brief assessment wherein a single dataset is excluded at a given time. This assessment was conducted in Tokyo, Osaka, and Aichi, and the learning period was from April 1, 2020 to June 30, 2021. Three time periods were included to demonstrate the spread (cases are increasing), peak (cases are at high values), and decay (cases are decreasing) of cases.

Discussion

In the early months of the COVID-19 pandemic, it was possible to estimate the DPC using only a small number of factors; however, after considering large-scale vaccination campaigns and the emergence of different variants, DPC estimation has become complicated. Regarding vaccination effectiveness, the effect of vaccination is not direct; hence, it needs to be carefully modeled by considering the variations in the vaccine type and potential waning of protection. Here, we present a method where the vaccination effect in one country can be projected to another country. For new viral variants, it is crucial to model its infectivity to correctly estimate such that the trigger of new wave and potential peak can be correctly estimated.

We studied forecasting using different setoff inputs that demonstrate varied factors discussed in the literature such as public mobility and behavior, meteorological data, vaccination effectiveness, and viral variant infectivity. The results demonstrate that different parameters have different implications along a given time course. Therefore, the training data should be carefully selected to obtain highly accurate long-term forecasts. We presented a feasible method to project the vaccination effectiveness obtained from another country and a model to manage the change in the infectivity of viral variants. As many countries have vaccination rates still below the target threshold for herd immunity set by the World Health Organization, it would be useful to validate the potential risks and forecast future waves of infection using data from other regions with high vaccination rates.

Ethics and permissions

No ethical permissions were needed in this study (numerical study with open data).

Role of the funding source

The funders of the study had no role in the study design, data collection, analysis, interpretation, preparation of the manuscript, or decision to publish.

References

1. Wouters OJ, et al. Challenges in ensuring global access to COVID-19 vaccines: production, affordability, allocation, and deployment. *The Lancet* 2021; 397: 1023-34.
2. Machingaidze S, Wiysonge CS. Understanding COVID-19 vaccine hesitancy. *Nature Med* 2021;27(8):1338-9.
3. Lurie N, Saville M, Hatchett R, Halton J. Developing Covid-19 vaccines at pandemic speed. *N Engl J Med* 2020;382(21):1969-73.
4. Mizrahi, B., Lotan, R., Kalkstein, N. et al. Correlation of SARS-CoV-2-breakthrough infections to time-from-vaccine. *Nature Commun* 2021;12:6379.
5. Wadman M. A grim warning from Israel: Vaccination blunts, but does not defeat Delta. *Science* 2021;373(6557):838-9.
6. Khoury DS, Cromer D, Reynaldi A, Schlub TE, Wheatley AK, Juno JA, et al. Neutralizing antibody levels are highly predictive of immune protection from symptomatic SARS-CoV-2 infection. *Nat Med* 2021;27:1205-1211.
7. Sanderson, K. COVID vaccines protect against Delta, but their effectiveness wanes. *Nature* 2021 (doi: <https://doi.org/10.1038/d41586-021-02261-8>).
8. Pouwels KB, Pritchard E, Matthews PC, Stoesser N, Eyre DW, Vihta K-D, et al. Effect of Delta variant on viral burden and vaccine effectiveness against new SARS-CoV-2 infections in the UK. *Nature Med* 2021;27(12):2127-35.
9. Cohn BA, Cirillo PM, Murphy CC, Krigbaum NY, Wallace AW. Breakthrough SARS-CoV-2 infections in 620,000 US Veterans, *medRxiv*. 2021 (doi: <https://doi.org/10.1101/2021.10.13.21264966>).
10. Japanese Cabinet Secretariat. COVID-19 AI & Simulation Project (<https://www.covid19-ai.jp/en-us>).
11. IHME COVID-19 Forecasting Team. Modeling COVID-19 scenarios for the United States. *Nature Med* 2021;27:94-105
12. He S, Peng Y, Sun K. SEIR modeling of the COVID-19 and its dynamics. *Nonlinear Dyn* 2020;101(3):1667-80.
13. Carcione JM, Santos JE, Bagaini C, Ba J. A simulation of a COVID-19 epidemic based on a deterministic SEIR model. *Front Pub Health* 2020;8:230.
14. Zeroual A, Harrou F, Dairi A, Sun Y. Deep learning methods for forecasting COVID-19 time-Series data: A Comparative study. *Chaos Soliton Fract*. 2020;140:110121.
15. Ardabili SF, Mosavi A, Ghamisi P, Ferdinand F, Varkonyi-Koczy AR, Reuter U, et al. Covid-19 outbreak prediction with machine learning. *Algorithms*. 2020;13(10):249.
16. Chang S, Pierson E, Koh PW, Gerardin J, Redbird B, Grusky D, et al. Mobility network models of COVID-19 explain inequities and inform reopening. *Nature*. 2021;589(7840):82-7.
17. Rashed EA, Hirata A. One-Year Lesson: Machine Learning Prediction of COVID-19 Positive Cases with Meteorological Data and Mobility Estimate in Japan. *Int J Env Res Pub He* 2021;18(11):5736.
18. Nikparvar, B., Rahman, M.M., Hatami, F. et al. Spatio-temporal prediction of the COVID-19 pandemic in US counties: modeling with a deep LSTM neural network. *Sci Rep* 2021;11:21715.
19. Rashed EA, Hirata A. Infectivity Upsurge by COVID-19 viral variants in Japan: Evidence from deep learning modeling. *Int J Env Res Pub He* 2021;18(15):7799.
20. Wintachai P, Prathom K. Stability analysis of SEIR model related to efficiency of vaccines for COVID-19 situation. *Helyon* 2021;7(4):e06812.
21. Benenson S, Oster Y, Cohen MJ, Nir-Paz R. BNT162b2 mRNA Covid-19 vaccine effectiveness among health care workers. *N Engl J Med* 2021;384(18):1775-7.
22. Zeng B, Gao L, Zhou Q, Yu K, Sun F. Effectiveness of COVID-19 vaccines against SARS-CoV-2 variants of concern: a systematic review and meta-analysis. *medRxiv* 2021 (<https://doi.org/10.1101/2021.09.23.21264048>)
23. Reis BY, Barda N, Leshchinsky M, Kepten E, Hernán MA, Lipsitch M, et al. Effectiveness of BNT162b2 vaccine against delta variant in adolescents. *N Engl J Med* 2021; 385(22): 2101-3
24. Aran D. Estimating real-world COVID-19 vaccine effectiveness in Israel using aggregated counts. *MedRxiv*. 2021

- (<https://doi.org/10.1101/2021.02.05.21251139>).
- 25. Bergwerk M, Gonen T, Lustig Y, Amit S, Lipsitch M, Cohen C, et al. Covid-19 breakthrough infections in vaccinated health care workers. *N Engl J Med.* 2021;385(16):1474-84.
 - 26. Pfizer and BioNTech Announce Phase 3 Trial Data Showing High Efficacy of a Booster Dose of Their COVID-19 Vaccine [press release]. 2021.
 - 27. Majumder P, Ray PP. A systematic review and meta-analysis on correlation of weather with COVID-19. *Scientific Reports.* 2021;11(1):1-10

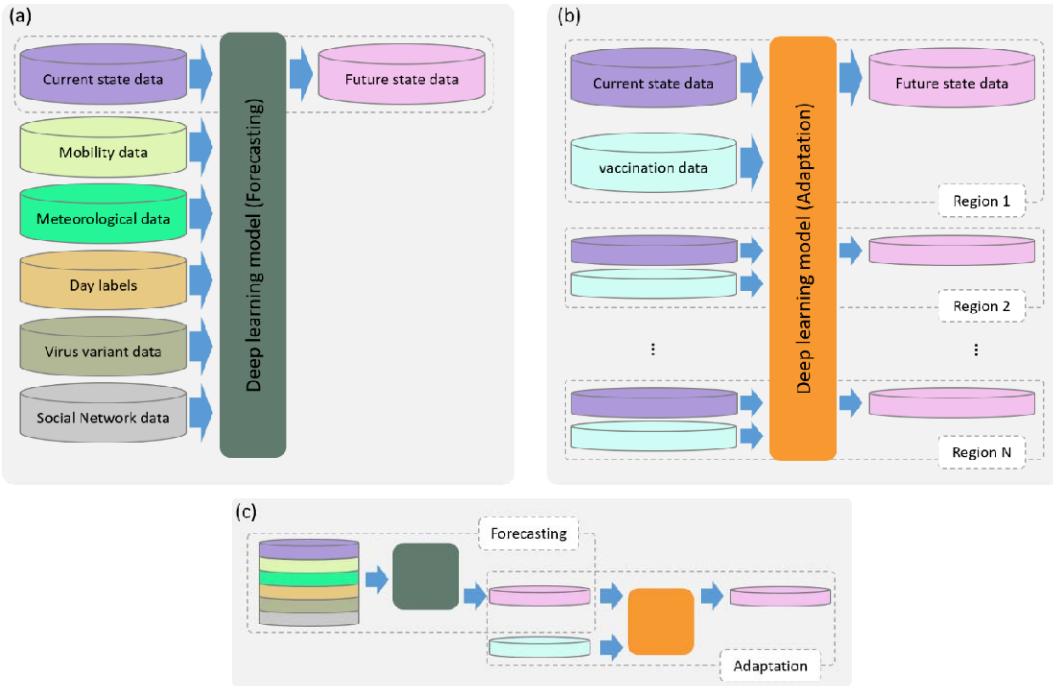


Figure 1: Outline of proposed model for COVID-19 status forecasting with vaccination effectiveness. (a) Initial forecasting is computed using a blend of time-serious data; (b) the vaccination effect is computed using data acquired from different regions; and (c) the full model includes steps in (a) forecasting and (b) adaptation.

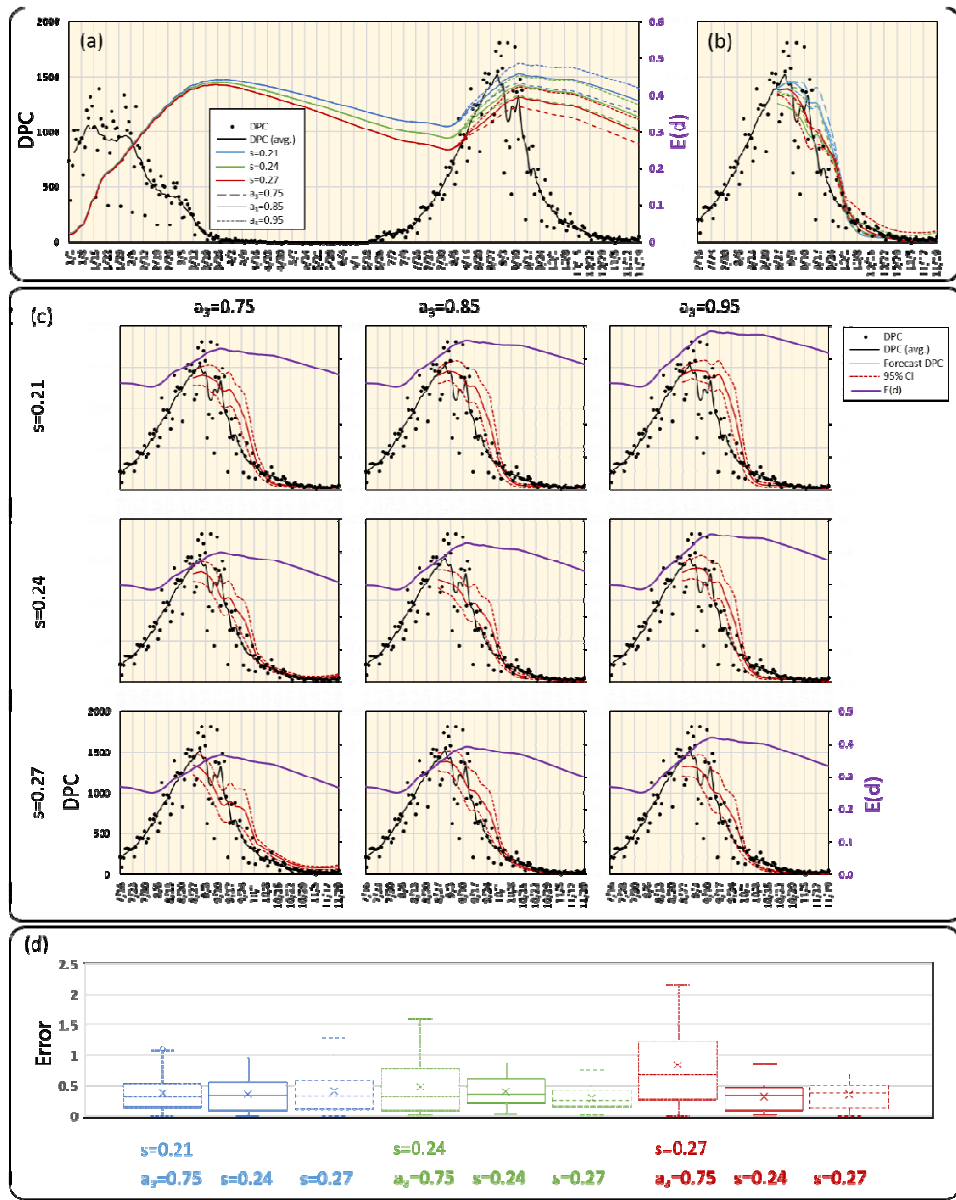


Figure 2: (a) Vaccination effectiveness model (Eq. 1) in Tel Aviv with different values of s and along with DPC. (b) Forecasted DPC (7-day average) using different vaccination effectiveness models during the decay of the COVID-19 wave. (c) Detailed forecasted DPC data including the 95% confidence interval and associated vaccination effectiveness model. (d) Error associated with the forecasts using different vaccination effectiveness models.

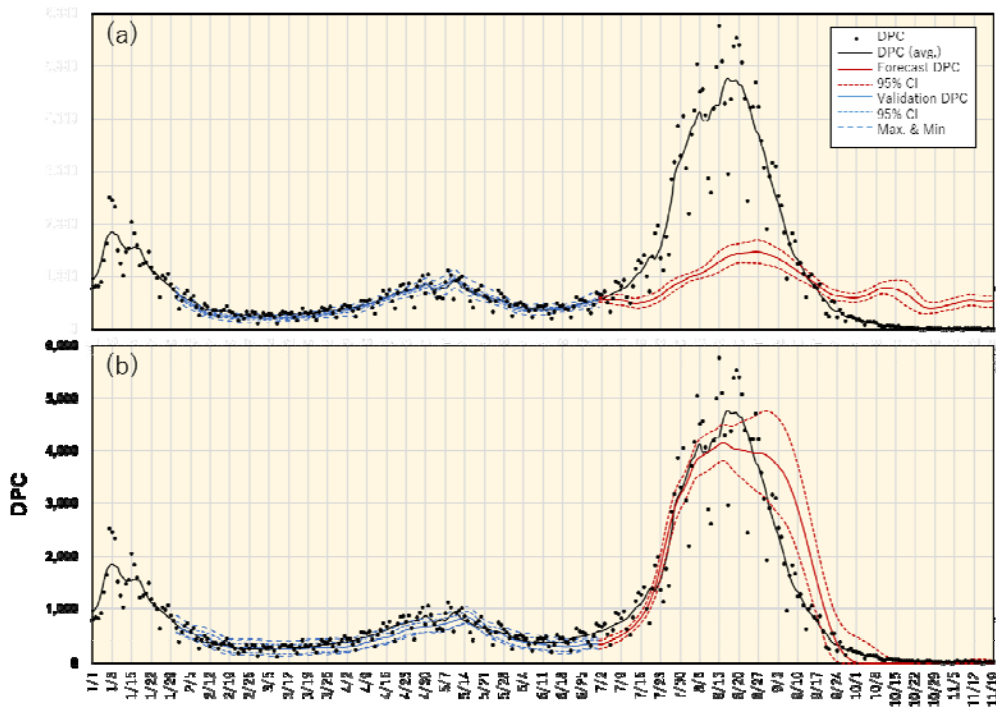


Figure 3: Predicted DPC in Tokyo for the fifth wave with (a) all datasets (included in Table S1) and (b) optimized datasets (only values of 1-1, 2-4, 5-1, 6-1, 7-1 from Table S1) along with true values. Training data are from August 1, 2020 to July 30, 2021.

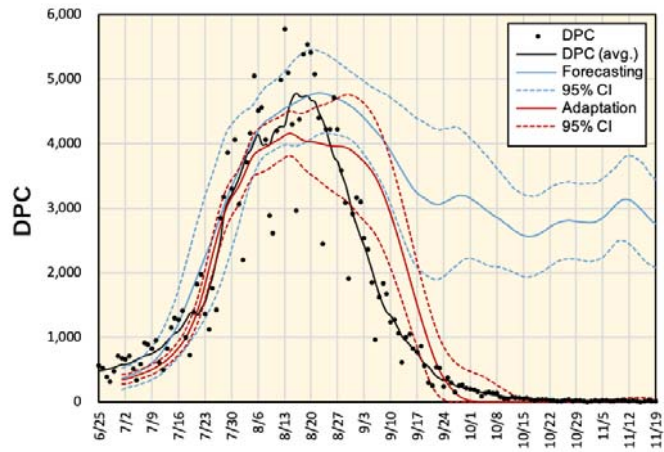


Figure 4: Comparison of forecasting and adaptation models (shown in Fig. 1) for DPC in Tokyo. This demonstrates the effect of vaccination, which shows a weak spread phase and prolonged decay phase of the fifth COVID-19 wave.

Table 1: Errors computed in the forecasts of separate phases of the fifth COVID-19 wave in Tokyo, Osaka, and Aichi with different data sets. Each experiment was conducted by excluding a single dataset (1-7) in Table S1. “None” demonstrates the case wherein all datasets are used, and “Optimized” demonstrates the best scenario. Green and red colors are the lowest and highest error values, respectively.

		Ex.1	Ex.2	Ex.3	Ex.4	Ex.5	Ex.6	Ex.7	None	Optimized*
Tokyo	Spread**	0.48	0.30	0.26	0.18	0.41	0.53	0.43	0.44	0.23
	Peak	0.64	0.61	0.45	0.56	0.74	0.65	0.63	0.68	0.09
	Decay	0.79	1.06	1.88	0.63	0.39	0.61	0.78	0.53	0.78
	Full Wave	0.63	0.65	0.85	0.46	0.52	0.62	0.61	0.55	0.36
Osaka	Spread	0.21	0.39	0.25	0.26	0.38	0.41	0.35	0.38	0.24
	Peak	0.82	0.76	0.69	0.56	0.82	0.75	0.73	0.75	0.09
	Decay	0.55	0.44	0.42	0.52	0.36	0.37	0.33	0.63	0.41
	Full Wave	0.51	0.53	0.45	0.45	0.52	0.53	0.47	0.58	0.24
Aichi	Spread	0.83	0.15	0.71	0.20	0.71	0.48	0.14	0.17	0.13
	Peak	0.86	0.75	0.55	0.79	0.55	0.44	0.49	0.49	0.16
	Decay	0.95	0.85	0.96	0.65	0.85	0.92	1.08	0.60	0.21
	Full Wave	0.88	0.58	0.74	0.54	0.70	0.60	0.57	0.42	0.17

* optimized inputs are 1-1, 2-4, 5-1, 6-1, 7-1 (see Table S1)

** spread (July), peak (August), decay (September), and all wave (July–September)

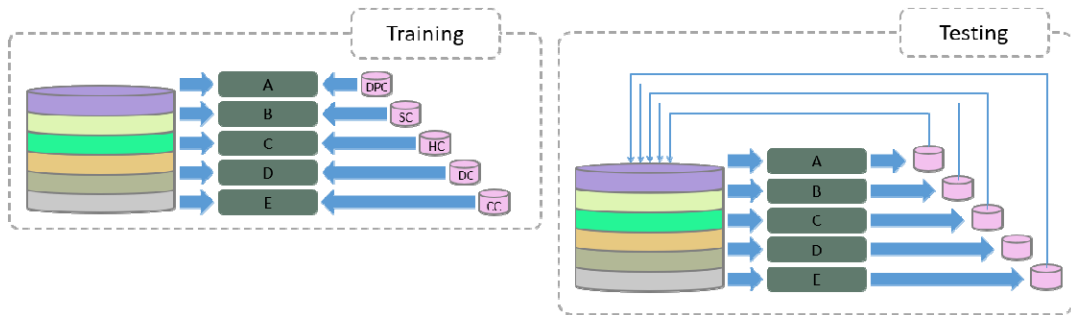


Figure S1: Training and testing phases for the COVID-19 forecasting model. In training, different networks (A–E) are trained to forecast specific status indicators. Long-term forecasting is achieved in the testing phase with concurrent data updates.



Figure S2: Map of Japan with study areas and regions used to represent downtown districts.

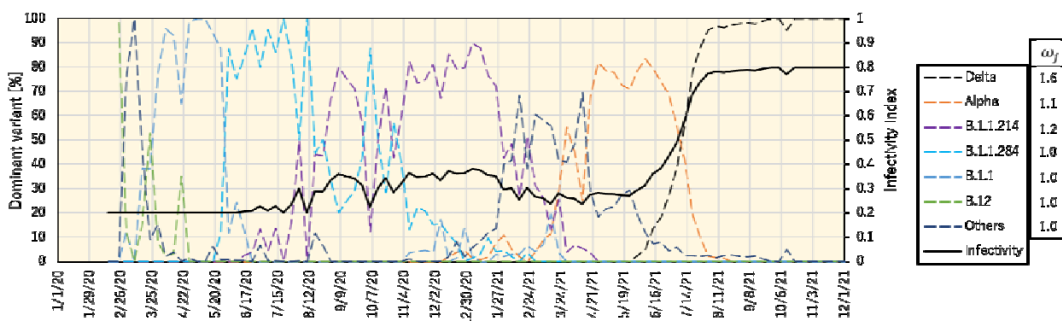


Figure S3: Example of a variant infectivity index computed using data of viral variant measures in Tokyo with associated weight values representing relative infectivity.

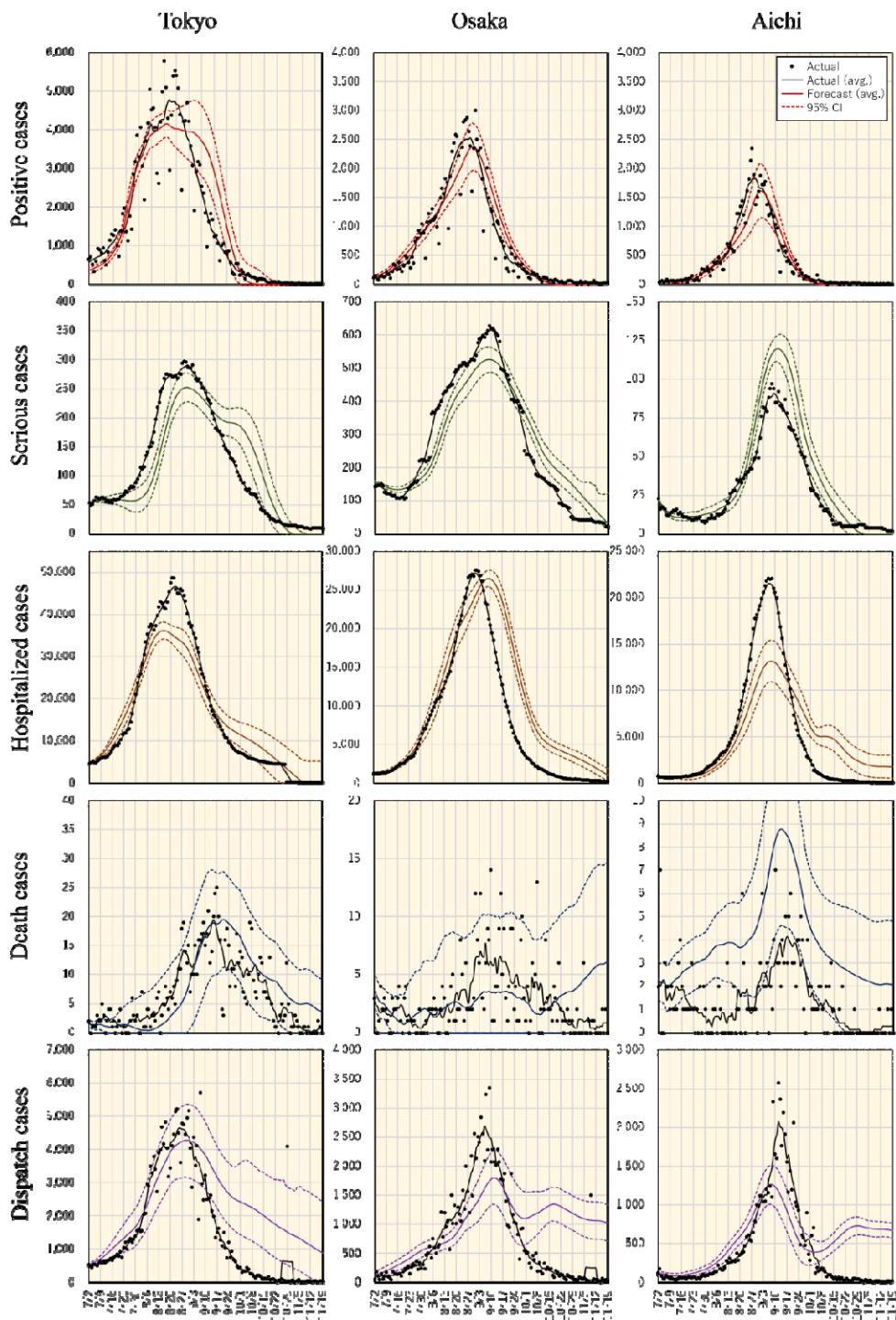


Figure S4: Forecasting future pandemic states for Tokyo, Osaka, and Aichi, considering the positive cases, serious cases, hospitalized cases, deaths, and hospital dispatch cases.

Table S1: Datasets used in the forecasting/adaptation models shown in Figure 1.

Dataset	Items	Scale
1-Current state data	1–1 Positive cases 1–2 Serious cases 1–3 Hospitalized cases 1–4 Death cases 1–5 Hospital discharged cases	Daily number of cases
2-Mobility data	2–1 Retail & recreation 2–2 Grocery & pharmacy 2–3 Parks 2–4 Transit stations 2–5 Workplaces 2–6 Residential 2–7 Downtown area population	Percent change from baseline (pre-pandemic)
3-Meteorological data	3–1 Maximum temperature 3–2 Minimum temperature 3–3 Average humidity	Daily value
4-Day labels	4–1 Working/holiday/ext. holiday 4–2 Normal/State of emergency	Labels (0/1/2)
5-Variant infectivity	5–1 $\tilde{f}(d)$	Computed using Eq. (3)
6-Behaviour	6–1 Tweets (“nomikai”) 6–2 Tweets (“karaoke”) 6–3 Tweets (“BBQ”) 6–4 Downtown area population	Daily tweets using keywords Daily number of persons
7-Vaccination effectiveness	7–1 $E(d)$	Computed using Eq. (1)